Fracture Failure Mechanism Analysis of Steel Bolt

Lei Guo [a], Yan Liu and Jiasheng Liu

The 713th Research Institute of CSSC, Zhengzhou 450015, China

[a] guol19880418@126.com

Abstract. In order to find out the cause of fracture failure of 08F steel bolt, the composition, macro and micro fracture morphology, microhardness and metallographic of the fractured part were observed and analyzed by means of scanning electron microscope, carbon sulfur analyzer, full spectrum direct reading plasma emission spectrometer, metallographic microscope, microhardness instrument and gas analyzer. The results show that the metallurgical quality of bolt material is normal, and the failure of the wheel hub bolt is the overload fracture when tightening the bolt.

Keywords: 08F Steel; Bolt; Fracture Morphology.

1. Introduction

08F steel is a high-quality carbon structural steel. It has higher strength than 05F steel, and has good plasticity, toughness and weldability. It is often used to manufacture various mechanical parts with high toughness requirements[1,2]. Aiming at the fracture phenomenon of wheel hub bolt during pre-tightening, the chemical composition, macro and micro fracture morphology, microhardness and metallographic of the broken bolt are observed and tested with the help of scanning electron microscope, carbon sulfur analyzer, full spectrum direct reading plasma emission spectrometer, metallographic microscope, microhardness instrument, gas analyzer and other equipment[3,4]. A comprehensive analysis of bolt fracture failure is carried out .

2. Analysis Process and Results

2.1 Chemical Composition Analysis

Samples were taken from three different positions of the broken bolt and their chemical composition was analyzed by ICP full spectrum direct reading plasma emission spectrometer and CS800 carbon sulfur analyzer. The measurement results are shown in Table 1. The results show that the chemical composition of the bolt meets the composition requirements of 08F steel in GB / T 699-1999 [5].

Table 1. Chemical composition of failure bolt(wt%)

	C	Si	Mn
Standard value	0.05-0.11	<=0.03	0.25-0.5
Sample 1	0.072	0.0120	0.386
Sample 2	0.073	0.0139	0.358
Sample 3	0.067	0.0083	0.330

2.2 Macroscopic Fracture Morphology Observation

The macro morphology of bolt fracture is shown in Figure 1. The fracture is located at the first thread where the nut and thread are not screwed. The section has a slight vortex feature, and no evidence of corrosion, original crack, obvious machining damage and other defects are found on the fracture surface. In addition, judging from the appearance of the bolt, the bolt may be formed by cold heading process.



Fig 1. Macroscopic fracture morphology

2.3 Micro Fracture Morphology Observation

The fracture (with nut end) was observed under the scanning electron microscope, and the fracture surface was in a slight vortex shape, as shown in Fig. 2(a). Under high power microscope, the fracture is characterized by dimple fracture. Except for the unclear direction of dimples in the center of vortex fracture, dimples in other areas are elongated and show the characteristics of shear dimples. The convergence position in the parabola direction where the dimple is elongated is the crack source area, the center of the vortex fracture is the final fracture area, and other areas are the crack propagation area, as shown in Fig. 2(a). No original cracks, inclusions and other metallurgical defects were found in the crack source area, and the fracture morphology is characterized by shear dimple, as shown in Fig. 2(b). The crack propagation area is characterized by shear dimple as a whole, as shown in Fig. 2(c), and the corresponding position of Fig. 2(c) is shown at "c" of Fig. 2(a) . The center of the vortex fracture is the final fracture area, the fracture is dimple fracture, and the dimple directivity is not obvious, as shown in Fig. 2(d). In addition, the shear dimples in the crack source region and propagation region are elongated in a rotation direction, which matches the direction of bolt tightening. No typical fatigue fracture morphology such as evidence of corrosion and fatigue striations was found on the section, and there were no typical hydrogen embrittlement features such as white spots and chicken feet patterns.

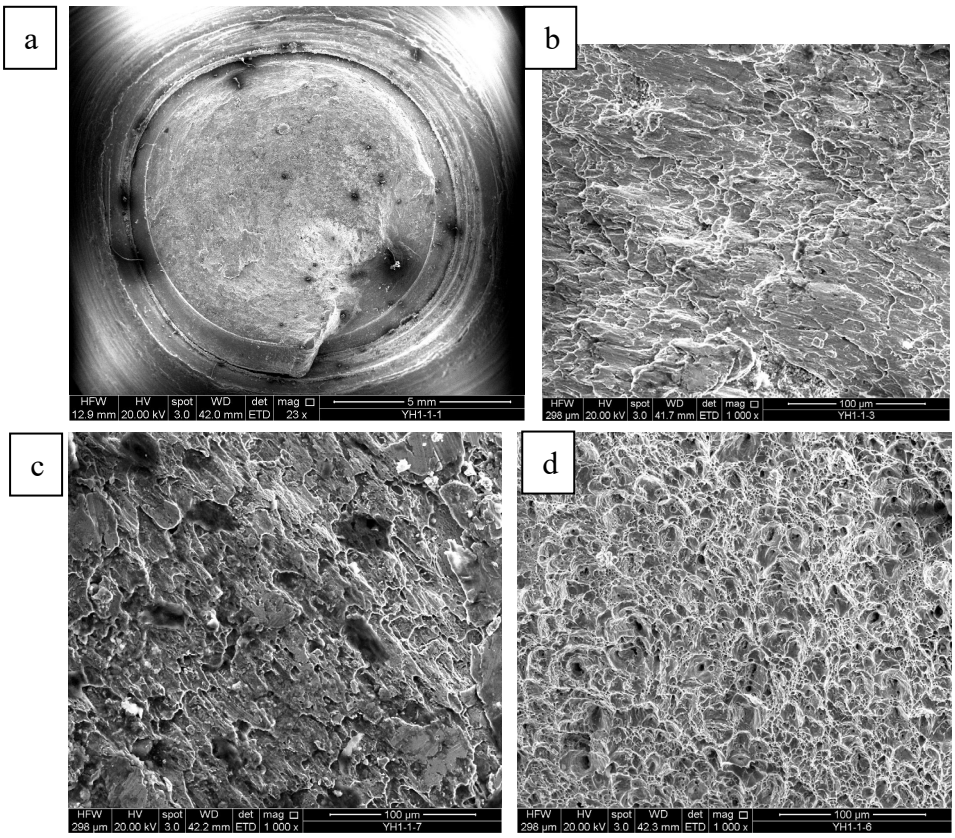


Fig 2. Micro morphology of fracture

2.4 Microhardness

The VMH-I04 microhardness tester was used to test the microhardness (308HV0.1) of the center of the cross section of the sample [6], the results are shown in Table 2.

Table 2. Microhardness test results

Serial number	1	2	3	4	5	Average value
1#	268	252	264	259	266	262
2#	223	205	217	192	219	211
3#	217	203	201	211	205	207

2.5 Metallographic Observation

Using metallographic microscope to conduct metallographic analysis on the longitudinal section of the fractured bolt, the morphology of the non-metallic inclusions is shown in Figure 3. The evaluation results of non-metallic inclusions are as follows: Category C and Level 2.5, Category D and Level 1.5 [7].

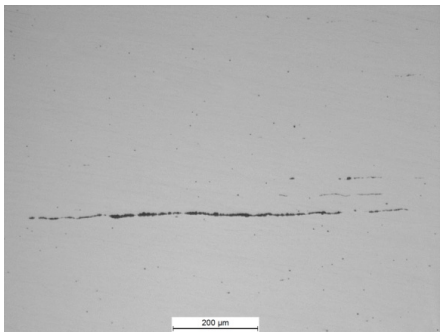


Fig 3. Non-metallic inclusions of the bolt

Samples 1, 2 and 3 all have ferrite and pearlite structures, among which the pearlite content of sample 1 is relatively large, and the morphology of the structure is shown in Figure 4.

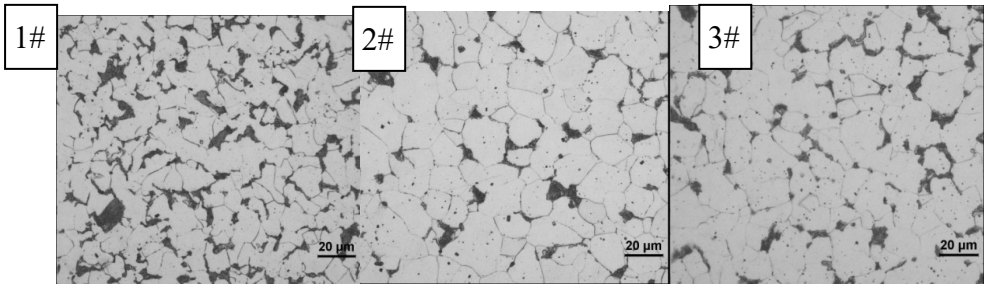


Fig 4. Metallographic structure 500×

There is no significant difference in the grain size of the three groups of samples. The grain size of the sample 1 is 11, the grain size of the sample 2 and sample 3 is 10.5, the grain size morphology is shown in Figure 5.

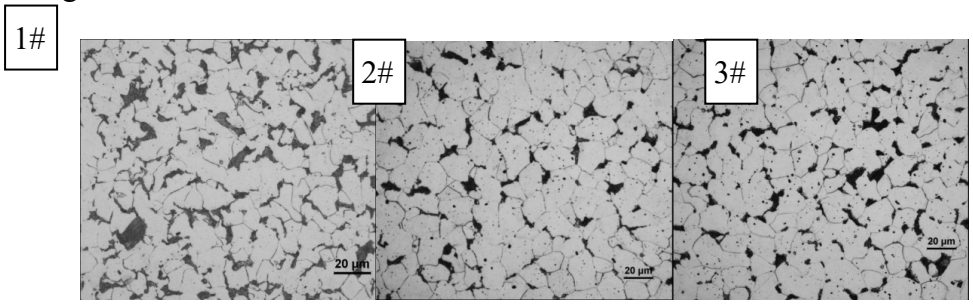
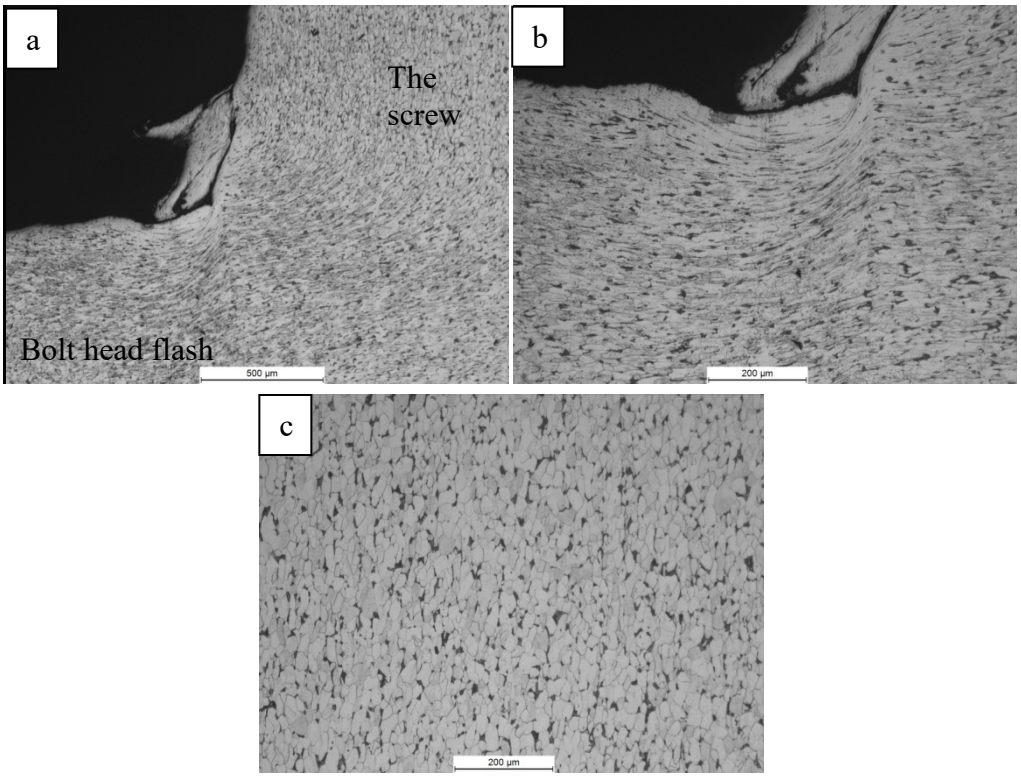


Fig 5. Grain size 500×

The longitudinal metallographic morphology of the sample is shown in Fig. 6. It can be seen that the grains at the flash of the bolt head and the position adjacent to the screw are elongated, and the grain elongation directions are perpendicular to each other, as shown in Fig. 6(a). The flash tissue of the bolt head is elongated horizontally, as shown in Fig. 6 (b). The screw tissue is elongated longitudinally, as shown in Fig. 6 (c).



(a) Overall structure morphology (b) Structure morphology of the flash of head (c) Structure morphology of the screw

Fig 6. Longitudinal metallographic structure of the hub bolt

3. Analysis and Discussion

3.1 Metallographic and Microhardness Analysis

The inclusion content of the broken bolt is Category C, Level 2.5 and Category D, Level 1.5. The inclusion content is not high, indicating that the metallurgical quality of the material is normal. The metallographic structure of the bolt is ferrite and pearlite, and the bolt material is annealed or normalized. The longitudinal metallographic structure of the broken bolt shows that the grains at the flash of the bolt head and the position adjacent to the screw are elongated,and the grain elongation directions are perpendicular to each other, indicating that the bolt is formed by cold heading process. The pearlite content and microhardness of sample 1 are relatively high, which may be related to the cooling rate during annealing or normalizing. When the cooling rate is too fast, it is easy to form a pseudo-eutectoid structure, resulting in higher hardness.

3.2 Fracture Analysis

No corrosion trace, original crack and obvious machining damage were found on the surface of the fracture, which indicates that the failure of the hub bolt is not caused by corrosion, original crack and machining damage defects. No obvious inclusions and other metallurgical defects were found in the crack source area, which shows that the failure of the wheel hub bolts is not caused by metallurgical quality problems. No typical hydrogen embrittlement features such as white spots and

chicken feet patterns were found, and the fracture was characterized by ductile fracture as a whole, and the H content was only 1.2ppm, indicating that the failure of the hub bolt has nothing to do with hydrogen embrittlement.

The fracture surface shows a slight vortex shape. Except that the direction of the dimple in the center of the vortex fracture is unclear, the dimples in other areas are elongated and show the characteristics of shear dimple, which is consistent with the overload fracture characteristics under the condition of static torsional stress. During the tightening process of the bolt, the stress is the largest at the first thread that is not screwed, which is consistent with the fact that the fracture is located at the first thread where the nut is not screwed with the bolt. The elongated direction of the shear dimple matches the direction of the bolt when it is tightened, which further indicates that the fracture of the bolt is the overload fracture when the bolt is tightened.

4. Conclusion

Based on the above analysis, the following conclusions can be drawn:

(1) The material of the wheel hub bolt is 08F steel, and the metallurgical quality of the material is normal;

(2) The forming process of the hub bolt is cold heading, and the heat treatment state of the bolt material is annealed or normalized.

(3) The failure of the wheel hub bolt is the overload fracture when the bolt is tightened.

References

[1] Lin Xin-bo, Xiao Hong-sheng, Zhang Zhi-liang, et al. The Experimental Research and Mathematical Modeling of 08F Steel Flow Stress in the Temperature Range of Warm forging. Journal of Plasticity Engineering. Vol. 8 (2001) No. 4, p. 1-5.

[2] Huang Ke, Ding Ren-hua, Ma Xue-feng, et al. Forging Process of Generator Claw Pole for Steel 08F. Forging & Stamping Technology. Vol. 43 (2018) No. 7, p. 129-132.

[3] Yin Hong-chao, Zhao Yun, Wang Xian-si, et al. Bolt Fracture Failure Analysis. Physics Examination and Testing. Vol. 35 (2017) No. 6, p. 30-32.

[4] Guo Chen, Zhang Ren-qi. The Failure Analysis of High Temperature Bolt Fracture of Steam Turbine. Guangdong Science & Technology. (2013) No. 20, p. 27-28.

[5] Cheng Da-xian. Handbook of Mechanical Design. Chemical Industry Press, 2016, p. 3-14.

[6] Yang Hao-quan, Zhou Ping. Study on the Characteristic of the Surface Microhardness For 45 Steel During High Cycle Fatigue. Physical Testing and Chemical Analysis(Part A:Physical Testing). Vol. 42 (2006) No. 7, p. 328-331.

[7] Li Hong-guang, Chen Tian-ming, Chen Liang, et al. Analysis and Research on The Segregation of A-type Inclusion in Rail Steel. Iron Steel Vanadium Titanium. Vol. 38 (2017) No. 2, p. 143-146.